Can Full-Duplex Jamming Reduce the Energy-Cost of a Secure Bit?

Omid Taghizadeh*, Peter Neuhaus†, Rudolf Mathar*
* Institute for Theoretical Information Technology, RWTH Aachen University, Aachen, 52074, Germany
† Vodafone Chair Mobile Communications Systems, Technische Universität Dresden, Dresden 01062, Germany
Email: {taghizadeh, mathar}@ti.rwth-aachen.de, peter.neuhaus@ifn.et.tu-dresden.de.

***Abstract*—In this work we study the secrecy energy efficiency (SEE) of a multiple-input-multiple-output multiple-antenna eavesdropper (MIMOME) wiretap channel, in terms of the securely communicated bits-per-Joule, where the legitimate receiver is equipped with full-duplex (FD) capability. In particular, we seek answer to the question: if and how the application of an FD jammer can enhance the system SEE, considering the additional power consumption used for jamming and self-interference cancellation, as well as the degrading effect of residual self-interference. In this regard, an SEE maximization problem is formulated. Due to the intractable problem structure, an iterative solution is provided with a guaranteed convergence to a local optimum. Moreover, the proposed solution is extended for a system with a bidirectional communication, where both legitimate nodes are equipped with FD capability. Numerical simulations indicate a marginal SEE gain, via the utilization of FD jamming, for a wide range of system conditions. However, the observed gain is significant for the scenarios with a small distance between the FD node and the eavesdropper, a high signal-to-noise ratio (SNR) condition or for a bidirectional FD communication setup, under the condition that the self-interference can be effectively and efficiently mitigated.**

***Keywords*—Full-duplex, friendly jamming, secrecy capacity, wiretap channel, energy efficiency, MIMO.**

I. Introduction

Full-duplex transceivers are capable of transmission and reception at the same time and frequency, however, suffering from a strong self-interference. Recently, practical implementations of FD transceivers have been achieved, employing advanced analog/digital signal processing methods for the purpose of self-interference cancellation [1], [2], thereby motivating studies regarding the applications of FD transceivers [3]. In particular, the application of FD transceivers is known to enhance the information security of wireless communication systems due to the capability to transmit jamming, i.e., an artificial noise (AN) signal, to the illegitimate receivers while exchanging information. The problems regarding secrecy rate region analysis and resource optimization has hence been addressed for the systems with FD capability in [4]–[8]. It is observed that a significant gain is achievable, in terms of the secrecy capacity[1], via the utilization of an FD jamming strategy under the condition that the self-interference signal can be attenuated effectively. However, the aforementioned improvement comes at the expense of a higher power consumption used for jamming, for the implementation of a self-interference cancellation scheme, as well as the degrading effect of the residual self-interference. Hence, it is not clear how the application of an FD jammer impact the secrecy energy efficiency, in terms of the securely communicated bits per-energy unit.

[1]Secrecy capacity is the maximum information rate that can be communicated under perfect secrecy, i.e., without being accessible by the illegitimate receivers [9].

A. Contribution

In this work we study the SEE maximization problem for a MIMOME wiretap channel, where Alice and an FD Bob are jointly capable of transmitting AN. Our main contributions are as following:

- In contrast to the available designs [5]–[8], utilizing FD transceivers for secrecy capacity enhancement, in Section III, an SEE maximization problem is formulated. Due to the intractable structure, a successive general inner approximation algorithm (SUIAP) is proposed, with a guaranteed convergence to a point satisfying Karush-Kuhn-Tucker (KKT) conditions of optimality.
- The joint utilization of FD capability, both on Alice and Bob for jamming and bi-directional information exchange, shows additional potentials for the improvement of SEE. This is grounded on the fact that *i)* the FD jamming power is reused for both communication directions, resulting in a power-efficient jamming, and *ii)* the coexistence of two communication directions on the same channel may degrade Eve's decoding capability. Motivated by this, the proposed SUIAP algorithm is extended in Section IV for an FD bidirectional setup.

The numerical results show that the utilization of FD transceivers is able to provide a significant SEE gain for a system with a small distance between the FD node and the eavesdropper, a high signal-to-noise ratio (SNR) or for a bidirectional FD communication setup, under the condition that the self-interference can be effectively and efficiently mitigated.

B. Mathematical notation

Throughout this paper, the Kronecker product is denoted by $\otimes$. The identity matrix with dimension K is denoted as $\mathbf{I}_K$. $\mathrm{diag}(\cdot)$ returns a diagonal matrix by putting the off-diagonal elements to zero. $\perp$ denotes statistical independence. The set of positive real numbers, the set of complex numbers, and the set of all positive semi-definite matrices with Hermitian symmetry are denoted by $\mathbb{R}^+$, $\mathbb{C}$ and $\mathcal{H}$, respectively. The value of $\{x\}^+$ is equal to x, if positive, and zero otherwise. Furthermore, $\mathcal{CN}(\mathbf{x}, \mathbf{X})$ denotes the complex normal distribution with mean $\mathbf{x}$ and covariance $\mathbf{X}$.

II. System Model

We consider a MIMOME wiretap channel that consists of a legitimate transmitter, i.e., Alice, a legitimate receiver, i.e., Bob, and an eavesdropper, i.e., Eve, see Fig. 1. Alice and Eve are equipped with N_A transmit and M_E receive antennas, respectively. Bob is respectively equipped with N_B and M_B transmit and receive antennas, and is capable of FD operation. Channels are assumed to follow a quasi-stationary[2]

[2]It means that the channel remains constant within a frame, but may change from one frame to another.

and flat-fading model. In this regard, channel from Alice to Bob, Alice to Eve, and Bob to Eve (jamming channel) are respectively denoted as $\mathbf{H}_{ab} \in \mathbb{C}^{M_B \times N_A}$, $\mathbf{H}_{ae} \in \mathbb{C}^{M_E \times N_A}$, $\mathbf{H}_{be} \in \mathbb{C}^{M_E \times N_B}$. The channel from Bob to Bob, i.e., self-interference channel, is denoted as $\mathbf{H}_{bb} \in \mathbb{C}^{M_B \times N_B}$.

A. Signal model

The transmission from Alice includes the information-containing signal, intended for Bob, and an AN, intended to degrade the reception by Eve. This is expressed as

$$\mathbf{x}_a = \underbrace{\mathbf{q}_a + \mathbf{w}_a}_{\mathbf{u}_a} + \mathbf{e}_{\text{tx},a}, \tag{1}$$

where $\mathbf{u}_a \in \mathbb{C}^{N_A}$ is the intended transmit signal, $\mathbf{q}_a \sim \mathcal{CN}(\mathbf{0}_{N_A}, \mathbf{Q}_a)$ and $\mathbf{w}_a \sim \mathcal{CN}(\mathbf{0}_{N_A}, \mathbf{W}_a)$ respectively represent the information-containing and AN signal, and $\mathbf{x}_a \in \mathbb{C}^{N_A}$ is the combined transmitted signal from Alice. The transmit distortion, denoted as $\mathbf{e}_{\text{tx},a} \in \mathbb{C}^{N_A}$ models collective impact of transmit chain inaccuracies, e.g., analog-to-digital converters (ADC) noise, power amplifier (PA) noise, oscillator phase noise, see Subsection II-B for more details. Note that the role of hardware inaccuracies becomes important in a system with FD transceivers, due to the impact of a strong self-interference channel. Similar to the transmission from Alice, the transmission of AN by Bob is expressed as

$$\mathbf{x}_b = \mathbf{w}_b + \mathbf{e}_{\text{tx},b}, \tag{2}$$

where $\mathbf{w}_b \sim \mathcal{CN}(\mathbf{0}_{N_B}, \mathbf{W}_b)$ is the transmitted artificial noise and $\mathbf{e}_{\text{tx},b} \in \mathbb{C}^{N_B}$ represents the transmit distortions from Bob. Via the application of (1) and (2) the received signal at Eve is expressed as

$$\begin{aligned} \mathbf{y}_e &= \mathbf{H}_{ae}\mathbf{x}_a + \mathbf{H}_{be}\mathbf{x}_b + \mathbf{n}_e, \\ &= \mathbf{H}_{ae}\mathbf{q}_a + \mathbf{c}_e \end{aligned} \tag{3}$$

where $\mathbf{n}_e \sim \mathcal{CN}\left(\mathbf{0}_{M_E}, \sigma^2_{\text{n},e}\mathbf{I}_{M_E}\right)$ is the additive thermal noise and

$$\mathbf{c}_e := \mathbf{H}_{ae}\mathbf{w}_a + \mathbf{H}_{be}\mathbf{w}_b + \mathbf{H}_{ae}\mathbf{e}_{\text{tx},a} + \mathbf{H}_{be}\mathbf{e}_{\text{tx},b} + \mathbf{n}_e \tag{4}$$

is the collective interference-plus-noise at Eve.

Similarly, the received signal at Bob is formulated as

$$\mathbf{y}_b = \underbrace{\mathbf{H}_{ab}\mathbf{x}_a + \mathbf{H}_{bb}\mathbf{x}_b + \mathbf{n}_b}_{=:\mathbf{u}_b} + \mathbf{e}_{\text{rx},b}, \tag{5}$$

where $\mathbf{n}_b \sim \mathcal{CN}\left(\mathbf{0}_{M_B}, \sigma^2_{\text{n},b}\mathbf{I}_{M_B}\right)$ is the additive thermal noise, and $\mathbf{u}_b$ is the received signal, assuming perfect hardware operation. Similar to the transmit side, the receiver distortion, denoted as $\mathbf{e}_{\text{rx},b} \in \mathbb{C}^{M_B}$, models the collective impact of receiver chain inaccuracies, e.g., digital-to-analog converter (DAC) noise, oscillator phase noise, and automatic gain control error, see Subsection II-B. Note that $\mathbf{y}_b$ includes the received self-interference signal at Bob, originating from the same transceiver. Hence, the *known*, i.e., distortion-free, part of the self-interference can be subtracted applying an SIC method [1], [2]. The received signal at Bob, after the application of SIC is hence written as

$$\begin{aligned} \tilde{\mathbf{y}}_b &= \mathbf{y}_b - \mathbf{H}_{bb}\mathbf{w}_b \\ &= \mathbf{H}_{ab}\mathbf{x}_a + \mathbf{H}_{bb}\mathbf{e}_{\text{tx},b} + \mathbf{e}_{\text{rx},b} + \mathbf{n}_b \\ &= \mathbf{H}_{ab}\mathbf{q}_a + \mathbf{c}_b, \end{aligned} \tag{6}$$

where

$$\mathbf{c}_b := \mathbf{H}_{ab}\mathbf{w}_a + \mathbf{H}_{ab}\mathbf{e}_{\text{tx},a} + \mathbf{H}_{bb}\mathbf{e}_{\text{tx},b} + \mathbf{e}_{\text{rx},b} + \mathbf{n}_b, \tag{7}$$

is the collective interference-plus-noise at Bob.

B. Distortion signal statistics

Similar to [10], we model the impact of transmit (receive) chain inaccuracies by injecting Gaussian-distributed and independent distortion terms at each antenna. Moreover, the variance of the distortion signals are proportional to the power of the intended transmit (receive) signal at the corresponding chain. This is expressed in our system as

$$\mathbf{e}_{\text{tx},a} \sim \mathcal{CN}\Big(\mathbf{0}_{N_A}, \kappa_a \text{diag}\Big(\mathbb{E}\left\{\mathbf{u}_a\mathbf{u}_a^H\right\}\Big)\Big), \quad \mathbf{e}_{\text{tx},a} \perp \mathbf{u}_a, \tag{10}$$

$$\mathbf{e}_{\text{tx},b} \sim \mathcal{CN}\Big(\mathbf{0}_{N_B}, \kappa_b \text{diag}\Big(\mathbb{E}\left\{\mathbf{w}_b\mathbf{w}_b^H\right\}\Big)\Big), \quad \mathbf{e}_{\text{tx},b} \perp \mathbf{w}_b, \tag{11}$$

$$\mathbf{e}_{\text{rx},b} \sim \mathcal{CN}\Big(\mathbf{0}_{M_B}, \beta_b \text{diag}\Big(\mathbb{E}\left\{\mathbf{u}_b\mathbf{u}_b^H\right\}\Big)\Big), \quad \mathbf{e}_{\text{rx},b} \perp \mathbf{u}_b, \tag{12}$$

where $\kappa_a, \kappa_b, \beta_b \in \mathbb{R}^+$ are distortion coefficients, relating the variance of the distortion terms to the intended signal power, and $\mathbf{u}_a$ and $\mathbf{u}_b$ are defined in (1) and (5), respectively. For further elaborations on the used distortion model please see [10], [11], and the references therein.

C. Power consumption model

The consumed power for Alice and Bob can be hence expressed as

$$P_A = \frac{1}{\mu_A}\mathbb{E}\left\{\|\mathbf{x}_a\|_2^2\right\} + P_{A,0}, \quad P_A \leq P_{A,\max} \tag{13}$$

and

$$P_B = \frac{1}{\mu_B}\mathbb{E}\left\{\|\mathbf{x}_b\|_2^2\right\} + P_{B,0} + P_{\text{FD}}, \quad P_B \leq P_{B,\max}. \tag{14}$$

In the above arguments, $P_{\mathcal{X}}, P_{\mathcal{X},0}, \mu_{\mathcal{X}}$, and $P_{\mathcal{X},\max}$, where $\mathcal{X} \in \{A, B\}$, respectively represent the consumed power, the zero-state power[3], PA efficiency, and the maximum allowed power consumption for each node. The additional required power for the implementation of an SIC scheme is denoted by P_{FD}. From (13), (14), the total system power consumption is obtained as

$$P_{\text{tot}} = P_A + P_B. \tag{15}$$

D. Secrecy energy efficiency

Following [4], [12], [13], the achievable secrecy rate[4] for Alice-Bob communication is expressed as $C_{ab} = \left\{\tilde{C}_{ab}\right\}^+$, such that

$$\tilde{C}_{ab} = \log\left|\mathbf{I} + \mathbf{H}_{ab}\mathbf{Q}_a\mathbf{H}_{ab}^H\mathbf{\Sigma}_b^{-1}\right| - \log\left|\mathbf{I} + \mathbf{H}_{ae}\mathbf{Q}_a\mathbf{H}_{ae}^H\mathbf{\Sigma}_e^{-1}\right|, \tag{16}$$

where $\mathbf{\Sigma}_b$, $\mathbf{\Sigma}_e$ are given in (8), (9), and represent the covariance of the interference-plus-noise terms at Bob and Eve, respectively. The secrecy energy efficiency (SEE), as a measure of securely communicated information per energy unit, is consequently expressed as

$$\text{SEE} = \frac{C_{ab}}{P_{\text{tot}}}. \tag{17}$$

It is the intention of the remaining parts of this paper to improve the efficiency of the defined wiretap channel, in terms of the SEE, and provide comparison to the usual HD strategies.

[3]The power consumed regardless of transmission, e.g., due to digital processing, power consumed at the receiver chain.

[4]The system secrecy capacity is lower bounded by all achievable secrecy rates resulting from different choices of transmit covariance matrices, see [13, Theorem 1], [12, Equation (6)].

$$\boldsymbol{\Sigma}_b = \mathbb{E}\{\mathbf{c}_b\mathbf{c}_b^H\} = \mathbf{H}_{ab}\mathbf{W}_a\mathbf{H}_{ab}^H + \kappa_a\mathbf{H}_{ab}\text{diag}\left(\mathbf{Q}_a + \mathbf{W}_a\right)\mathbf{H}_{ab}^H + \kappa_b\mathbf{H}_{bb}\text{diag}\left(\mathbf{W}_b\right)\mathbf{H}_{bb}^H + \beta_b\text{diag}\Big(\mathbf{H}_{ab}\left(\mathbf{Q}_a + \mathbf{W}_a\right)\mathbf{H}_{ab}^H + \mathbf{H}_{bb}\mathbf{W}_b\mathbf{H}_{bb}^H + \sigma_{\text{n},b}^2\mathbf{I}_{M_B}\Big) + \sigma_{\text{n},b}^2\mathbf{I}_{M_B}, \quad (8)$$

$$\boldsymbol{\Sigma}_e = \mathbb{E}\{\mathbf{c}_e\mathbf{c}_e^H\} = \mathbf{H}_{ae}\mathbf{W}_a\mathbf{H}_{ae}^H + \mathbf{H}_{be}\mathbf{W}_b\mathbf{H}_{be}^H + \kappa_a\mathbf{H}_{ae}\text{diag}\left(\mathbf{Q}_a + \mathbf{W}_a\right)\mathbf{H}_{ae}^H + \kappa_b\mathbf{H}_{be}\text{diag}\left(\mathbf{W}_b\right)\mathbf{H}_{be}^H + \sigma_{\text{n},e}^2\mathbf{I}_{M_E}. \quad (9)$$

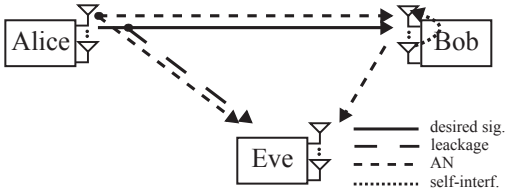

Figure 1. The studied wiretap channel. Alice, and the FD-Bob are jointly enabled with jamming capability.

III. Secrecy Energy Efficiency Maximization

In this part we intend to enhance the system SEE, assuming the availability of CSI for all channels. The corresponding optimization problem is defined as

$$\max_{\mathbf{Q}_a,\mathbf{W}_a,\mathbf{W}_b} \quad \text{SEE}\left(\mathbf{Q}_a,\mathbf{W}_a,\mathbf{W}_b\right) \quad (19a)$$

$$\text{s.t.} \quad \frac{1+\kappa_a}{\mu_a}\text{tr}\left(\mathbf{Q}_a+\mathbf{W}_a\right) + P_{A,0} \leq P_{A,\max}, \quad (19b)$$

$$\frac{1+\kappa_b}{\mu_b}\text{tr}\left(\mathbf{W}_b\right) + P_{B,0} + P_{\text{FD}} \leq P_{B,\max}, \quad (19c)$$

$$\mathbf{Q}_a,\mathbf{W}_a,\mathbf{W}_b \in \mathcal{H}, \quad (19d)$$

where (19b) and (19c) represent the power constraints at Alice and Bob, see (13), (14). The defined problem in (19) is not tractable in the current form, due to the non-convex and non-smooth objective. In order to obtain a tractable structure, without loss of optimality, we remove the non-linear operator $\{\}^+$ from the definition of SEE[5]. The modified SEE, named SEE_p hereinafter, can hence be formulated as

$$\text{SEE}_p\left(\mathbf{Q}_a,\mathbf{W}_a,\mathbf{W}_b\right) = \frac{\Sigma_{\mathcal{X}\in\{b,e\}}\alpha_{\mathcal{X}}\left(\log\left|\boldsymbol{\Sigma}_{\mathcal{X}}+\mathbf{H}_{a\mathcal{X}}\mathbf{Q}_a\mathbf{H}_{a\mathcal{X}}^H\right| - \log\left|\boldsymbol{\Sigma}_{\mathcal{X}}\right|\right)}{P_{\text{tot}}\left(\mathbf{Q}_a,\mathbf{W}_a,\mathbf{W}_b\right)}, \quad (20)$$

where $\alpha_b = 1$ and $\alpha_e = -1$. It is observed that SEE_p is a difference of concave (DC) over affine fractional function which is intractable in the current form. In the following we propose a successive general inner approximation algorithm (SUIAP) to obtain an optimal solution to (19).

A. SUIAP

The proposed SUIAP algorithm consists of two nested loops. In each outer iteration, an effective lower bound to SEE_p is constructed following the successive inner approximation (SIA) method [15], applying the inequality

$$-\log\left|\mathbf{X}\right| \geq -\log\left|\mathbf{Y}\right| + \text{tr}\left(\mathbf{Y}^{-1}\left(\mathbf{Y}-\mathbf{X}\right)\right) \quad (21)$$

as the first-order Taylor approximation of the convex terms $-\log|\cdot|$ in (20) at the point $\mathbf{Y}$. Please note that via the elimination of the convex terms from the nominator, the proposed lower bound holds a concave over affine fractional structure, which is a psedu-concave function [16]. Hence, in the inner loop, the well-known Dinkelbach's algorithm [17] can be applied to iteratively maximize the obtained lower bound. The proposed SUIAP algorithm, for the lth outer iteration and kth inner iteration is hence formulated as

$$\max_{\mathbb{Q}^{[k,l]}} \quad \tilde{\text{SEE}}_p\left(\mathbb{Q}^{[k,l]},\mathbb{Q}^{[0,l]},\lambda^{[k-1,l]}\right) \quad (22a)$$

$$\text{s.t.} \quad \text{(19b), (19c), (19d),} \quad (22b)$$

where $\mathbb{Q} := \{\mathbf{Q}_a,\mathbf{W}_a,\mathbf{W}_b\}$, $\tilde{\text{SEE}}_p$ is defined in (18), λ is an auxiliary variable, and $\boldsymbol{\Sigma}_b^{[k,l]}, \boldsymbol{\Sigma}_e^{[k,l]}$ are calculated from (8), (9) at the iteration instance represented by k,l.

It is observed that $\tilde{\text{SEE}}_p$ is a jointly concave function over $\mathbf{Q}_a^{[k,l]}, \mathbf{W}_a^{[k,l]}, \mathbf{W}_b^{[k,l]}$ for a fixed $\lambda^{[k,l]}$. In particular, the maximization over $\mathbb{Q}^{[k,l]}$ is efficiently implemented via the MAX-DET algorithm in each inner iteration, see [18]. Afterwards, in each inner algorithm iteration the value of $\lambda^{[k,l]}$ is uniquely updated by solving the identity

$$\tilde{\text{SEE}}_p\left(\mathbb{Q}^{[k,l]},\mathbb{Q}^{[0,l]},\lambda^{[k,l]}\right) = 0, \quad (23)$$

see [19, Subsection 3.2], [17] for more elaboration regarding the Dinkelbach's algorithm. The defined algorithm steps, both outer and inner loop iterations, are continued until a jointly stable point is obtained, see Algorithm 1 for more details.

B. Convergence

It is observed that the proposed steps in the inner loop lead to a necessary convergence, due to the monotonically increasing update of λ and the fact that a feasible value of λ is bounded from above. Moreover, it is proven in [19, Proposition 3.2] that for the studied concave-over-affine fractional structure, the converging point of the Dinkelbach's algorithm is indeed the global optimum point. The global optimality result of the inner loop iterations also results in a necessary convergence in the outer loop, by ensuring a monotonic improvement. Please note that the obtained lower bound via the utilization of (21) is a tight and global lower bound to SEE_p. Moreover, it shares the same slope as the SEE_p function at the point of approximation. The aforementioned properties, and the fact that inner iterations are solved to the optimality, results in the convergence of the outer loop iterations to a point satisfying the Karush-Kuhn-Tucker (KKT) conditions of the original problem, see [15, Theorem 1]. However, the converging KKT point of the original problem is not necessarily the global optimum. This optimality gap is numerically analyzed in Subsection V-A by examining multiple initializations.

C. Initialization

In order to obtain an efficient initialization we separate the design of spatial beams and power allocation for different transmissions, thereby obtaining a low-complexity but sub-optimal solution. The detailed initialization procedure is moved to [22] due to space limitations.

D. Computational complexity

The computational complexity of the algorithm is dominated by the steps of the determinant maximization in the inner

[5]Note that at the optimality of (19), the resulting C_{s}, and consequently the SEE is non-negative. This is since a non-negative SEE is immediately obtained by setting $\mathbf{Q}_a = \mathbf{0}$, see [4], [14] for similar arguments.

$$\tilde{\text{SEE}}_p\left(\mathbb{Q}^{[k,l]},\mathbb{Q}^{[0,l]},\lambda^{[k,l]}\right)=\log\left|\mathbf{\Sigma}_b^{[k,l]}+\mathbf{H}_{ab}\mathbf{Q}_a^{[k,l]}\mathbf{H}_{ab}^H\right|-\log\left|\mathbf{\Sigma}_b^{[0,l]}\right|+\text{tr}\left(\left(\mathbf{\Sigma}_b^{[0,l]}\right)^{-1}\left(\mathbf{\Sigma}_b^{[0,l]}-\mathbf{\Sigma}_b^{[k,l]}\right)\right)$$
$$+\log\left|\mathbf{\Sigma}_e^{[k,l]}\right|-\log\left|\mathbf{\Sigma}_e^{[0,l]}+\mathbf{H}_{ae}\mathbf{Q}_a^{[0,l]}\mathbf{H}_{ae}^H\right|+\text{tr}\left(\left(\mathbf{\Sigma}_e^{[0,l]}+\mathbf{H}_{ae}\mathbf{Q}_a^{[0,l]}\mathbf{H}_{ae}^H\right)^{-1}\left(\mathbf{\Sigma}_e^{[0,l]}-\mathbf{\Sigma}_e^{[k,l]}+\mathbf{H}_{ae}\left(\mathbf{Q}_a^{[0,l]}-\mathbf{Q}_a^{[k,l]}\right)\mathbf{H}_{ae}^H\right)\right)$$
$$-\lambda^{[k-1,l]}\left(\frac{1+\kappa_a}{\mu_a}\text{tr}\left(\mathbf{Q}_a^{[k,l]}+\mathbf{W}_a^{[k,l]}\right)+\frac{1+\kappa_b}{\mu_b}\text{tr}\left(\mathbf{W}_b^{[k,l]}\right)+P_{A,0}+P_{B,0}+P_{\text{FD}}\right) \quad (18)$$

loop, see Algorithm 1, Step 6. A general form of a MAX-DET problem is defined as

$$\min_{\mathbf{z}}\ \mathbf{p}^T\mathbf{z}+\log\left|\mathbf{Y}(\mathbf{z})^{-1}\right|,\ \text{ s.t. }\ \mathbf{Y}(\mathbf{z})\succ 0,\ \mathbf{F}(\mathbf{z})\succeq 0, \quad (24)$$

where $\mathbf{z}\in\mathbb{R}^n$, and $\mathbf{Y}(\mathbf{z})\in\mathbb{R}^{n_Y\times n_Y}:=\mathbf{Y}_0+\sum_{i=1}^n z_i\mathbf{Y}_i$ and $\mathbf{F}(\mathbf{z})\in\mathbb{R}^{n_F\times n_F}:=\mathbf{F}_0+\sum_{i=1}^n z_i\mathbf{F}_i$. An upper bound to the computational complexity of the above problem is given as

$$\mathcal{O}\Big(\gamma_{\text{in}}\sqrt{n}\big(n^2+n_Y^2\big)n_F^2\Big), \quad (25)$$

see [18, Section 10]. In our problem $n=2N_A^2-2N_A+N_B^2-N_B$ representing the dimension of real valued scalar variable space, and $n_Y=M_B+M_E$ and $n_F=N_B+2N_A+2$, representing the dimension of the determinant operation and the constraints space, respectively.

Algorithm 1 Successive inner approximation algorithm (SUIAP) for SEE maximization. $C_{\min}$ ($\lambda_{\min}$) represents the convergence threshold for the outer (inner) iterations.

1: $l,k\leftarrow 0$; $\lambda^{[0,0]}\leftarrow\mathbf{0},\mathbb{Q}^{[0,0]}\leftarrow$ Subsection III-C; ▷ initialization
2: **repeat** ▷ outer loop
3: $l\leftarrow l+1$,
4: $\lambda^{[0,l]}\leftarrow\lambda^{[k,l-1]}$; $\mathbb{Q}^{[0,l]}\leftarrow\mathbb{Q}^{[k,l-1]}$; $k\leftarrow 0$,
5: **repeat** ▷ inner loop (Dinkelbach alg.)
6: $k\leftarrow k+1$; $\mathbb{Q}^{[k,l]}\leftarrow$ MAX-DET [18], see (22);
7: $C\leftarrow\tilde{\text{SEE}}_p\left(\mathbb{Q}^{[k,l]},\mathbb{Q}^{[0,l]},\lambda^{[k,l]}\right)$; $\lambda^{[k,l]}\leftarrow$ (23);
8: **until** $C\leq C_{\min}$
9: **until** $\lambda^{[k,l]}-\lambda^{[0,l]}\leq\lambda_{\min}$
10: **return** $\left\{\mathbb{Q}^{[k,l]},\lambda^{[k,l]}\right\}$

IV. Secure Bidirectional Communication: Joint Full-Duplex Operation at Alice and Bob

In this part we study the case that a bidirectional communication is established between Alice and Bob, where both Alice and Bob are enabled with FD capability. An FD bidirectional setup is interesting as it enables the usage of the same channel for both communication directions, and leads to a higher spectral efficiency [10]. Moreover, the jamming power at both Alice and Bob can be reused to improve security at both directions[6], and potentially improve the resulting SEE. However, the coexistence of all signal transmissions on a single channel results in a higher number of interference paths, which calls for a smart design regarding the signal and jamming transmit strategies at Alice and Bob.

In order to update the defined setup to a bidirectional one, we denote the number of receive antennas, and the self-interference channel at Alice as M_A, $\mathbf{H}_{aa}$, respectively. Moreover, we denote that the data transmission from Bob as $\mathbf{q}_b\sim\mathcal{CN}(\mathbf{0}_{N_B},\mathbf{Q}_b)$. Following the same signal model for the transmission of data and jamming signals as in (1) - (12), the received interference-plus-noise covariance matrix at Bob and Eve are updated respectively as

$$\mathbf{\Sigma}_b^{\text{BD}}=\mathbf{\Sigma}_b+\kappa_b\mathbf{H}_{bb}\text{diag}\left(\mathbf{Q}_b\right)\mathbf{H}_{bb}^H+\beta_b\text{diag}\left(\mathbf{H}_{bb}\mathbf{Q}_b\mathbf{H}_{bb}^H\right), \quad (26)$$

$$\mathbf{\Sigma}_e^{\text{BD}}=\mathbf{\Sigma}_e+\kappa_b\mathbf{H}_{be}\text{diag}\left(\mathbf{Q}_b\right)\mathbf{H}_{be}^H, \quad (27)$$

[6]This is since the jamming sent to Eve from each single node degrades Eves reception quality from both communication directions.

where $\beta_a\in\mathbb{R}^+$ is the distortion coefficient for the reception at Alice. Please note that in the formulation of (27) we consider a worst-case scenario where the interference on Eve, due to the transmission of data signals, i.e., $\mathbf{q}_a$ and $\mathbf{q}_b$, can be decoded [20]. Similarly, the received interference-plus-noise signal covariance at Alice is written as

$$\mathbf{\Sigma}_a^{\text{BD}}=\mathbf{H}_{ba}\mathbf{W}_b\mathbf{H}_{ba}^H+\sigma_{\text{n},a}^2\mathbf{I}_{M_A}+\kappa_b\mathbf{H}_{ba}\text{diag}\left(\mathbf{Q}_b+\mathbf{W}_b\right)\mathbf{H}_{ba}^H$$
$$+\kappa_a\mathbf{H}_{aa}\text{diag}\left(\mathbf{W}_a+\mathbf{Q}_a\right)\mathbf{H}_{aa}^H+\beta_a\text{diag}\Big(\mathbf{H}_{ba}\left(\mathbf{Q}_b+\mathbf{W}_b\right)\mathbf{H}_{ba}^H$$
$$+\mathbf{H}_{aa}\left(\mathbf{W}_a+\mathbf{Q}_a\right)\mathbf{H}_{aa}^H+\sigma_{\text{n},a}^2\mathbf{I}_{M_A}\Big), \quad (28)$$

where $\sigma_{\text{n},a}^2$ represents the thermal noise variance at Alice. The SEE for the defined BD system is then obtained as

$$\text{SEE}^{\text{BD}}=\frac{\left\{\tilde{C}_{ab}\right\}^+ +\left\{\tilde{C}_{ba}\right\}^+}{P_{\text{tot}}}, \quad (29)$$

where $\tilde{C}_{ab}$ is obtained by applying (26), (27) into (17), and

$$\tilde{C}_{ba}=\log\Big|\mathbf{I}+\mathbf{H}_{ba}\mathbf{Q}_b\mathbf{H}_{ba}^H\left(\mathbf{\Sigma}_a^{\text{BD}}\right)^{-1}\Big|$$
$$-\log\Big|\mathbf{I}+\mathbf{H}_{be}\mathbf{Q}_b\mathbf{H}_{be}^H\left(\mathbf{\Sigma}_e^{\text{BD}}\right)^{-1}\Big|, \quad (30)$$

is defined similar to (16) but for the opposite direction.

Lemma IV.1. *The values $\tilde{C}_{ab}$ and $\tilde{C}_{ba}$ in the nominator of (29) are non-negative for an optimal choice of $\mathbf{Q}_a,\mathbf{Q}_b$, under some mild practical assumptions.*

Proof: The proof is moved to [22, Section IV] due to space limitations. ■

A. Extended SUIAP for bidirectional-SEE maximization

In the first step we remove the nonlinear operator $\{\}^+$ from the nominator of (29), following the result of Lemma IV.1, hence turning the BD-SEE objective into a DC over affine fraction. Moreover, it is observed that the SEE^{BD} maximization holds a similar mathematical structure in relation to the transmit covariance matrices, i.e., $\mathbf{Q}_{\mathcal{X}},\mathbf{W}_{\mathcal{X}}$, $\mathcal{X}\in\{a,b\}$ as addressed for (19). Hence, a similar procedure as in the SUIAP algorithm is employed to obtain an optimal solution, with a guaranteed convergence to a point satisfying KKT conditions. The computational complexity of each Dinkelbach step is obtained similar to (25), where $n=2N_A^2-2N_A+2N_B^2-2N_B$, $n_Y=M_B+M_A+M_E$ and $n_F=2N_B+2N_A+2$.

V. Simulation Results

In this section the performance of the studied MIMOME system is evaluated in terms of the resulting SEE, via numerical simulations. In particular, we are interested in a comparison between the performance of an FD-enabled setup, compared to the case where all nodes operate in HD mode. Moreover, the evaluation of the proposed SEE-specific designs is of interest, in comparison to the available designs which target the maximization of the system's secrecy capacity. We assume that all communication channels follow an uncorrelated Rayleigh flat-fading model with variance $\rho_{\mathcal{X}}=\bar{\rho}/d_{\mathcal{X}}^2$, where $d_{\mathcal{X}}$ is the link distance and depends on the simulated geometry,

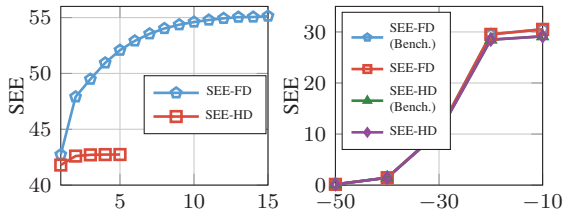

(a) Convergence (b) Init. (SUAIP)

Figure 2. Numerical algorithm analysis in terms of the average convergence behavior, initialization, and the optimality gap.

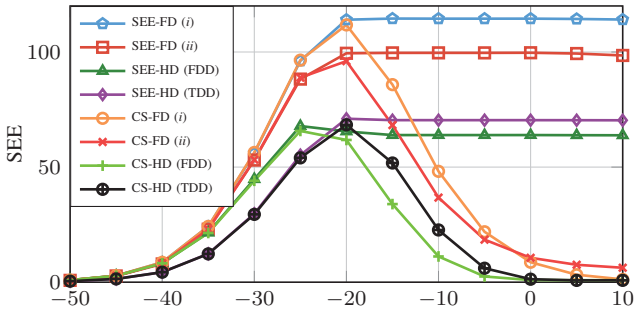

Figure 3. SEE performance of FD, FDD and TDD for secure bidirectional communications.

$\mathcal{X} \in \{ab, ba, ae, be\}$. For the self-interference channels we follow the characterization reported in [21]. In this respect we have $\mathbf{H}_{bb} \sim \mathcal{CN}\left(\sqrt{\frac{\rho_{\text{si}} K_R}{1+K_R}}\mathbf{H}_0, \frac{\rho_{\text{si}}}{1+K_R}\mathbf{I}_{M_B} \otimes \mathbf{I}_{N_B}\right)$, where ρ_{si} represents the self-interference channel strength, $\mathbf{H}_0$ is a deterministic term[7], and K_R is the Rician coefficient. The statistics of the self-interference channel on Alice, i.e., $\mathbf{H}_{aa}$, is defined similarly. The resulting system SEE is evaluated by employing different design strategies, and averaged over 100 channel realizations. Unless otherwise is stated, the default simulated setup is defined as follows: $P_{\max} := P_{\mathcal{X},\max} = 0$dB, $P_0 := P_{\mathcal{X},0} = -20$dB, $\mu := \mu_{\mathcal{X}} = 0.9$, $\kappa := \kappa_{\mathcal{X}} = \beta_{\mathcal{X}} = -40$dB, $N := N_{\mathcal{X}} = M_{\mathcal{X}} = 4$, $\mathcal{X}, \in \{A, B\}$. Moreover we set $P_{\text{FD}} = 0$, $\rho_{\text{si}} = 0$dB, $K_R = 10$, $\bar{\rho} = -20$dB, and $\sigma_{\text{n}}^2 := \sigma_{\text{na}}^2 = \sigma_{\text{nb}}^2 = \sigma_{\text{ne}}^2 = -40$dB. Three nodes are equidistantly positioned, with the distance equal to one[8].

A. Algorithm analysis

Due to the iterative structure of the proposed algorithms the convergence behavior of the algorithms are of high interest. In Fig. 2 (a) the average convergence behavior of the SUAIP algorithm is depicted. As expected, a monotonic objective improvement is observed, with convergence in 5-20 total outer iterations. In Fig. 2 (b), it is observed that the proposed initialization achieves a close performance to the optimal performance; the highest SEE obtained by repeating the SUIAP algorithm for several random initializations.

B. Performance comparison

In this part the SEE performance of the FD-enabled system is evaluated via the application of the proposed SUAIP algorithm, and under different system conditions. The following benchmarks are implemented to provide a meaningful comparison.

[7]For simplicity, we choose $\mathbf{H}_0$ as a matrix of all-1 elements.

[8]We consider unit-less parameters to preserve a general framework. However, the obtained SEE values can be interpreted as the number of securely communicated bits per-Hz per-Joule, assuming the power values are in Watt.

- *SEE-FD* (*SEE-HD*): The proposed SUAIP algorithm, assuming an FD (HD) Bob.
- *CS-FD* (*CS-FD*): The design with the intention of maximizing secrecy capacity. Bob is capable of FD (HD) operation.

In Figs. 4 (a) and (b) the impact of thermal noise variance and the available transmit power are depicted. It is observed that a higher σ_{n}^2 (lower $P_{\max}$) results in a smaller SEE both for FD and HD setups. Moreover, a visible gain for FD setup is obtained compared to the HD setup, for a system with a high SNR. This is expected, since FD jamming becomes less effective when Eve is already distorted with high thermal noise power.

In Fig. 4 (c) the impact of transceiver accuracy is depicted. As expected, a higher value of κ results in a smaller achievable SEE, both in HD and FD setups. Moreover, it is observed that FD jamming can be beneficial only for a system with an accurate hardware operation, due to the impact of residual self-interference. However, results show that targeting SEE as the design objective results in a significant energy efficiency gain, compared to the available designs which target the maximization of secrecy rate.

In Fig. 4 (d) the impact of Eve's distance to Alice (d_E) is depicted. It is assumed that three nodes are positioned in a line with a total Alice-Bob distance of 100, where Eve is positioned in between. It is observed that the system SEE increases as d_E increase, and Eve gets closer to Bob. Moreover, the application of FD jamming becomes beneficial only when Eve is located in a close distance to Bob, and hence the channel between Bob and Eve, i.e., the jamming channel, is strong.

In Figs. 4 (e) the impact of the number of antenna elements at Eve (M_E) on SEE is depicted. As expected, a larger M_E results in a reduced SEE as it results in a stronger Alice-Eve channel. Moreover, the application of an FD jammer becomes gainful for a higher values of M_E, in order to counteract the improved Eve reception capability. In Figs. 4 (f)-(h) the impact of the transceiver's power efficiency is evaluated on the resulting system SEE. In particular, the impact of the zero-state power consumption (P_0), PA efficiency (μ) and the additional power consumption for SIC (P_{FD}) are depicted respectively in Fig. 4 (f), (g) and (h). It is observed that higher (lower) values of μ (P_0, P_{FD}) result in a smaller SEE. Moreover, it is observed that a marginal gain with the application of an FD jammer is obtained for a high μ, and a small P_{FD} conditions. This is expected, since a small (large) value of μ (P_{FD}) results in a bigger waste of power when using an FD jamming strategy.

1) Secure bidirectional communication: In Fig. 3 a system with a bidirectional secure communication between Alice and Bob is studied. In particular, a joint FD operation at Alice and Bob is considered which enables jamming and communication simultaneously at both directions. Two scenarios are considered regarding the decoding capability at Eve: *i*) Eve treats interference from the non-intended information path as noise, and *ii*) Eve is capable of decoding, and hence reducing, the received signal from the non-intended information link. Moreover, a setup with HD Bob and HD Alice is also evaluated, where time-division-duplexing (TDD) or frequency-division-duplexing (FDD) is employed in order to facilitate a bidirectional communication. It is observed that the resulting SEE increases with $P_{\max}$, however, saturates for high values of maximum transmit power. Moreover, it is observed that a joint FD operation is capable of enhancing the system SEE, with a considerable margin, in the studied bidirectional setup. This is since, due to the coexistence of both communication directions

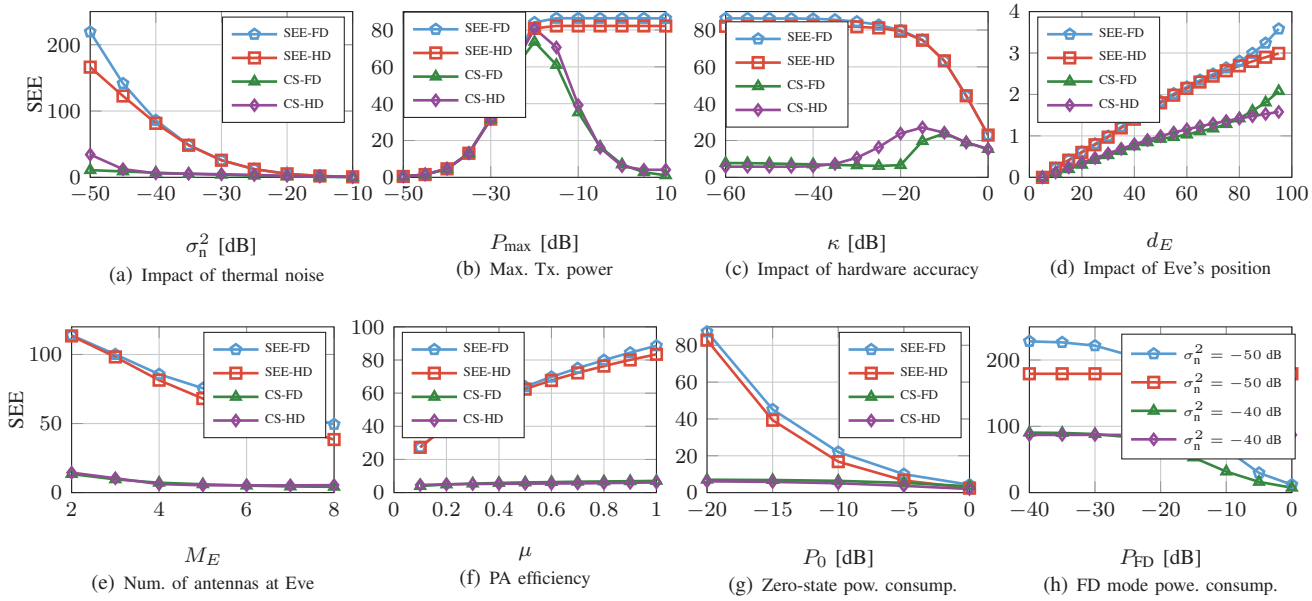

Figure 4. SEE performance of the secure communication system via the utilization of the SUAIP algorithm.

on the same channel the jamming power is re-used for both communication directions, leading to a higher SEE compared to the HD setup. Moreover, the Eve's decoding capability is further decreased in the FD setup considering the scenario (*i*), due to the existence of two information links at the same channel.

VI. Conclusion

The utilization of FD jamming transceivers is known to significantly enhance the secrecy capacity of wireless communication systems, by transmitting AN while exchanging information. However, this results in a higher power consumption due to jamming, and self-interference cancellation. In this work, we have observed that the application of FD transceivers result only in a marginal gain in terms of secrecy energy efficiency, for a wide range of system conditions. However, the aforementioned SEE gain becomes significant for a system with a small distance between the FD node to the eavesdropper, or a system operating in high SNR regimes, under the condition that the self-interference can be effectively and efficiently mitigated. Moreover, a promising SEE gain is observed for an FD bidirectional communication, where jamming power can be reused for both directions. It is observed that for almost all system conditions, the application of an SEE-aware design is essential, compared to the available designs which target the maximization of secrecy capacity.

References

[1] D. Bharadia and S. Katti, "Full duplex MIMO radios," in *Proceedings of the 11th USENIX Conference on Networked Systems Design and Implementation*, ser. NSDI'14, Berkeley, CA, USA, 2014.

[2] D. Bharadia, E. McMilin, and S. Katti, "Full duplex radios," in *Proceedings of the ACM SIGCOMM 2013 Conference on SIGCOMM*, ser. SIGCOMM '13. New York, NY, USA: ACM, 2013.

[3] A. Sabharwal, P. Schniter, D. Guo, D. W. Bliss, S. Rangarajan, and R. Wichman, "In-band full-duplex wireless: Challenges and opportunities," *IEEE Journal on Selected Areas in Communications*, Sep 2014.

[4] G. Zheng, I. Krikidis, J. Li, A. Petropulu, and B. Ottersten, "Improving physical layer secrecy using full-duplex jamming receivers," *IEEE Transactions on Signal Processing*, Oct 2013.

[5] L. Li, Z. Chen, D. Zhang, and J. Fang, "A full-duplex bob in the MIMO gaussian wiretap channel: Scheme and performance," *IEEE Signal Processing Letters*, Jan 2016.

[6] F. Zhu, F. Gao, M. Yao, and H. Zou, "Joint information- and jamming-beamforming for physical layer security with full duplex base station," *IEEE Transactions on Signal Processing*, Dec 2014.

[7] Y. Zhou, Z. Z. Xiang, Y. Zhu, and Z. Xue, "Application of full-duplex wireless technique into secure MIMO communication: Achievable secrecy rate based optimization," *IEEE Signal Processing Letters*, July 2014.

[8] B. Akgun, O. O. Koyluoglu, and M. Krunz, "Exploiting full-duplex receivers for achieving secret communications in multiuser miso networks," *IEEE Transactions on Communications*, Feb 2017.

[9] A. D. Wyner, "The wire-tap channel," *The Bell System Technical Journal*, Oct 1975.

[10] B. P. Day, A. R. Margetts, D. W. Bliss, and P. Schniter, "Full-duplex bidirectional MIMO: Achievable rates under limited dynamic range," *IEEE Transactions on Signal Processing*, July 2012.

[11] X. Xia, D. Zhang, K. Xu, W. Ma, and Y. Xu, "Hardware impairments aware transceiver for full-duplex massive MIMO relaying," *IEEE Transactions on Signal Processing*, Dec 2015.

[12] S. Goel and R. Negi, "Guaranteeing secrecy using artificial noise," *IEEE Transactions on Wireless Communications*, June 2008.

[13] F. Oggier and B. Hassibi, "The secrecy capacity of the MIMO wiretap channel," *IEEE Transactions on Information Theory*, Aug 2011.

[14] A. Zappone, P.-H. Lin, and E. Jorswieck, "Energy efficiency of confidential multi-antenna systems with artificial noise and statistical csi," *IEEE Journal of Selected Topics in Signal Processing*, 2016.

[15] B. R. Marks and G. P. Wright, "Technical note—a general inner approximation algorithm for nonconvex mathematical programs," *Operations Research*, 1978.

[16] E. Beckenbach *et al.*, "Generalized convex functions," *Bull. Amer. Math. Soc*, vol. 43, no. 6, pp. 363–371, 1937.

[17] W. Dinkelbach, "On nonlinear fractional programming," *Management science*, 1967.

[18] L. Vandenberghe, S. Boyd, and S.-P. Wu, "Determinant maximization with linear matrix inequality constraints," *SIAM Journal on matrix analysis and applications*, vol. 19, no. 2, pp. 499–533, 1998.

[19] A. Zappone, E. Jorswieck *et al.*, "Energy efficiency in wireless networks via fractional programming theory," *Foundations and Trends® in Communications and Information Theory*, 2015.

[20] D. W. K. Ng, E. S. Lo, and R. Schober, "Robust beamforming for secure communication in systems with wireless information and power transfer," *IEEE Transactions on Wireless Communications*, Aug 2014.

[21] M. Duarte, C. Dick, and A. Sabharwal, "Experiment-driven characterization of full-duplex wireless systems," *IEEE Transactions on Wireless Communications*, Dec 2012.

[22] O. Taghizadeh, P. Neuhaus, and R. Mathar, "Secrecy Energy Efficiency of MIMOME Wiretap Channels with Full-Duplex Jamming," *Pre-print, arXiv:1708.05402*, Aug. 2017.